International Scholarly Research Network
ISRN Signal Processing
Volume 2011, Article ID 683972, 7 pages
doi:10.5402/2011/683972

Research Article

Decoding of Turbo Codes in Symmetric Alpha-Stable Noise

Mohammad Shafieipour,[1,2] Heng-Siong Lim,[3] and Teong-Chee Chuah[1]

[1] *Faculty of Engineering, Multimedia University, Jalan Multimedia, 63100 Cyberjaya, Selangor, Malaysia*
[2] *Department of Electrical and Computer Engineering, University of Manitoba, Winnipeg, MB, Canada R3T 5V6*
[3] *Faculty of Engineering & Technology, Multimedia University, Jalan Ayer Keroh Lama, 75450 Melaka, Malaysia*

Correspondence should be addressed to Mohammad Shafieipour, m.shafieipour@mmu.edu.my

Received 7 December 2010; Accepted 27 January 2011

Academic Editors: A. Fernandez-Caballero and K. Sivakumar

This paper investigates the decoding of turbo codes in impulsive symmetric α-stable (SαS) noise. Due to the nonexistence of a closed-form expression for the probability density function (pdf) of α-stable processes, numerical-based SαS pdf is used to derive branch transition probability (btp) for the maximum *a posteriori* turbo decoder. Results show that in Gaussian noise, the turbo decoder achieves similar performance using both the conventional and the proposed btps, but in impulsive channels, the turbo decoder with the proposed btp substantially outperforms the turbo decoder utilizing the conventional btp. Results also confirm that the turbo decoder incorporating the proposed btp outperforms the existing Cauchy-based turbo decoder in non-Cauchy impulsive noise, while the two decoders accomplish similar performance in Cauchy noise.

1. Introduction

Turbo codes invented in 1993 [1] have many applications in various fields [2–4]. However, they were developed under the assumption of Gaussian noise despite the fact that many practical environments are known through experimental measurements to suffer from frequent occurrence of impulsive noise. Examples of such impulsive transmission links include radio channels [5], power-line communication channels [6], and digital subscriber lines [7]. Since systems optimized for Gaussian noise usually perform poorly in impulsive noise channels [8, 9], it is important to study and improve the performance of turbo codes in the presence of impulsive interference.

One commonly used impulsive noise model is the class of symmetric α-stable (SαS) distributions [10], of which the Gaussian and Cauchy distributions are special cases. This family possesses some desirable properties, but no closed-form expressions exist for their probability density function (pdf), except for the two limiting cases of Gaussian and Cauchy. Thus, previous studies have developed only noncoherent receivers based on the Gaussian and Cauchy pdfs. For uncoded systems, the authors in [11, 12] proposed Cauchy-based receivers to work in impulsive SαS noise. In [13], the authors studied soft-decision decoding in SαS noise based on the required side information. In their approach, Gaussian and Cauchy pdfs were used to derive closed-form soft-decision metrics which lead to exact receivers in Gaussian and Cauchy noise. The exact metrics were then simplified by averaging some parameters in order to lessen the required side information. It was then empirically shown that the exact Cauchy-based metric could outperform other metrics in impulsive SαS noise.

In this paper, we propose a new branch transition probability (btp) for the maximum *a posteriori* (MAP) turbo decoder which covers all cases of SαS noise including Gaussian and Cauchy. Unlike previous work where Cauchy-based receivers [11, 12] or closed-form Gaussian and Cauchy-based solutions [13] were suggested, the current work is based on the SαS pdf which is not available in closed form but is computed numerically.

The rest of this paper is organized as follows. In Section 2, we present the basic definitions and properties of SαS noise. In Section 3, a brief review of the turbo decoder is presented and the proposed numerical btp is described. In Section 4, the performance of the turbo decoder using the existing

analytical and the new numerical btps is compared through simulation results. Finally, the conclusions are drawn in Section 5.

2. SαS Noise

SαS random processes have been found to agree well with the measured data of a variety of man-made and natural noises [10], and this family possesses strong theoretical justifications according to the generalized central limit theorem. A random variable X follows a SαS distribution if its characteristic function has the following form:

$$\phi_X(\omega) = \exp(-\gamma|\omega|^\alpha), \quad -\infty < \omega < \infty, \tag{1}$$

where the parameter $\alpha \in (0, 2]$ is the characteristic exponent which determines the level of the impulsiveness of the SαS random process. A smaller value of α signifies a more impulsive behavior and vice versa. The scale parameter $\gamma > 0$ is called the dispersion which measures the spread of X. Note that when $\alpha = 2$, Gaussian noise is obtained with the following closed-form pdf:

$$f_2(\xi) = \frac{1}{2\sqrt{\pi\gamma}} \exp\left(-\frac{1}{4\gamma}\xi^2\right) \tag{2}$$

while $\alpha = 1$ leads to a Cauchy noise pdf

$$f_1(\xi) = \frac{\gamma}{\pi(\gamma^2 + \xi^2)}. \tag{3}$$

However, when $(0 < \alpha < 2,\ \alpha \neq 1, 2)$, no closed-form expressions exist for the pdf, but $f_\alpha(\xi)$ can be evaluated by taking the inverse Fourier transform of the characteristic function

$$f_\alpha(\xi) = \frac{1}{2\pi} \int_{-\infty}^{\infty} \exp(-\gamma|\omega|^\alpha) e^{-j\omega\xi} d\omega. \tag{4}$$

Due to the nonexistence of second- and higher-order moments for non-Gaussian SαS distributions, it is necessary to define an alternative measure for the power of SαS non-Gaussian noise. For this purpose, we use the E_b/N_0 for SαS noise defined in [14]

$$\frac{E_b}{N_0} = \frac{\text{GSNR}}{2rm}, \tag{5}$$

where r is the code rate, m is the number of bits carried per M-ary symbol ($m = 1$ for binary codes), and GSNR represents the geometric signal-to-noise ratio defined for non-Gaussian SαS noise [15].

3. Turbo Decoder

In this paper, we focus on the standard turbo code formed by two recursive systematic convolutional codes [1]. The general structure of the iterative turbo decoder is shown in Figure 1.

The two component decoders are linked by an interleaver and a deinterleaver. As shown in Figure 1, each component decoder accepts three inputs: (1) the systematically encoded channel output bits, (2) the parity bits transmitted from the respective component encoder, and (3) the information bits from the other component decoder for use as the prior information. The component decoders work iteratively to generate the *a posteriori* probability log-likelihood ratio (APP-LLR)

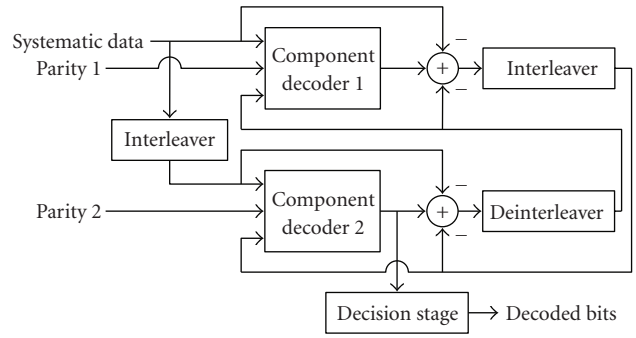

Figure 1: Turbo decoder structure.

$$L(u_k \mid \mathbf{y}) = \ln\left(\frac{P(u_k = +1 \mid \mathbf{y})}{P(u_k = -1 \mid \mathbf{y})}\right), \tag{6}$$

where $P(u_k = \pm 1 \mid \mathbf{y})$ is the APP of the kth data bit u_k, $k = 1, 2, \ldots, K$, and $\mathbf{y} = \mathbf{x} + \mathbf{n}$ is the noisy received codeword. We assume that u_k and the components of $\mathbf{x}$ take values in the set $\{\pm 1\}$ and $\mathbf{n}$ is the noise vector. The optimal solution to generate the APP-LLR can be obtained using the MAP algorithm which is also known as BCJR algorithm due to its inventors [16]. The MAP algorithm estimates (6) by incorporating the code's trellis

$$L(u_k \mid \mathbf{y}) = \ln\left(\frac{\sum_{U_k^+} P(s' \cap s \cap \mathbf{y})}{\sum_{U_k^-} P(s' \cap s \cap \mathbf{y})}\right), \tag{7}$$

where U_k^+ is the set of transitions from the previous state s' to the present state s caused by $u_k = +1$, and similarly for U_k^-. The joint probability $P(s' \cap s \cap \mathbf{y})$ in (7) can be decomposed into a product of three terms [1]

$$P(s' \cap s \cap \mathbf{y}) = P\left(y_{j>k} \mid s\right) \underbrace{P\{(y_k \cap s) \mid s'\}}_{\beta_k(s', s)} P\left(s' \cap y_{j<k}\right), \tag{8}$$

where $P(y_{j>k} \mid s)$ and $P(s' \cap y_{j<k})$ can be calculated recursively from the btp $\beta_k(s', s)$ [1]

$$\begin{aligned} \beta_k(s', s) &= P\{(\mathbf{y}_k \cap s) \mid s'\} \\ &= P\{\mathbf{y}_k \mid (s' \cap s)\} P(s \mid s') \\ &= P\{\mathbf{y}_k \mid (s' \cap s)\} P(u_k), \end{aligned} \tag{9}$$

where

$$P(u_k) = \left(\frac{e^{-L(u_k)/2}}{1 + e^{-L(u_k)}}\right) e^{(u_k L(u_k)/2)} \tag{10}$$

is the *a priori* probability of the data bit u_k, and $L(u_k) = \ln(P(u_k = +1)/P(u_k = -1))$ is its LLR. The term $P\{\mathbf{y}_k \mid (s' \cap s)\}$ in (9) is equivalent to $P(\mathbf{y}_k \mid \mathbf{x}_k)$, where $\mathbf{x}_k$ is the

transmitted codeword associated with the transition from s' to s. Thus, for a nonfading and memoryless channel with BPSK modulation, we can write

$$P\{\mathbf{y}_k \mid (s' \cap s)\} \equiv P(\mathbf{y}_k \mid \mathbf{x}_k) = \prod_{l=1}^{n} P(y_{kl} \mid x_{kl}) = \prod_{l=1}^{n} f(y_{kl} - x_{kl}), \tag{11}$$

where y_{kl} are the individual bits within the received codeword $\mathbf{y}_k$ and similarly for x_{kl} and f is the pdf of the additive noise. By substituting (10) and (11) into (9), the btp can be written as

$$\beta_k(s', s) = Ce^{(u_k L(u_k)/2)} \prod_{l=1}^{n} f(y_{kl} - x_{kl}), \tag{12}$$

where

$$C = \left(\frac{e^{-L(u_k)/2}}{1 + e^{-L(u_k)}} \right) \tag{13}$$

depends only on the LLR $L(u_k)$ and not on the sign of the data bit u_k or the transmitted codeword $\mathbf{x}_k$ and so is constant over the summations in the numerator and denominator in (7) and is canceled out.

3.1. The Gaussian btp. In the original MAP decoding algorithm, the btp is defined based on the Gaussian noise assumption. Thus, $f(y_{kl} - x_{kl})$ can be obtained using (2), and the Gaussian btp may be expressed as

$$\begin{aligned} \beta_{2,k}(s', s) &= Ce^{(u_k L(u_k)/2)} \prod_{l=1}^{n} f_2(y_{kl} - x_{kl}) \\ &= Ce^{(u_k L(u_k)/2)} \prod_{l=1}^{n} \frac{1}{2\sqrt{\pi\gamma}} \exp\left(-\frac{1}{4\gamma} (y_{kl} - x_{kl})^2 \right) \\ &= C_2 e^{(u_k L(u_k)/2)} \exp\left(\frac{1}{2\gamma} \sum_{l=1}^{n} y_{kl} x_{kl} \right), \end{aligned} \tag{14}$$

where the subscript 2 indicates the Gaussian ($\alpha = 2$) assumption and the constant term

$$C_2 = C \frac{1}{\left(2\sqrt{\pi\gamma}\right)^n} \exp\left(-\frac{1}{4\gamma} \sum_{l=1}^{n} \left(y_{kl}^2 + x_{kl}^2 \right) \right) \tag{15}$$

will be cancelled out in the calculation of (7). In this paper, the conventional MAP decoding algorithm is also called the Gaussian-based MAP decoder since it has the Gaussian btp in its structure.

3.2. The Cauchy btp. To modify the MAP algorithm to work in Cauchy noise, the Cauchy btp can be obtained in closed form based on the Cauchy pdf (3)

$$\begin{aligned} \beta_{1,k}(s', s) &= Ce^{(u_k L(u_k)/2)} \prod_{l=1}^{n} f_1(y_{kl} - x_{kl}) \\ &= Ce^{(u_k L(u_k)/2)} \prod_{l=1}^{n} \frac{\gamma}{\pi\left\{\gamma^2 + (y_{kl} - x_{kl})^2\right\}} \\ &= C_1 e^{(u_k L(u_k)/2)} \prod_{l=1}^{n} \frac{1}{\left\{\gamma^2 + (y_{kl} - x_{kl})^2\right\}}, \end{aligned} \tag{16}$$

where the subscript 1 indicates the Cauchy ($\alpha = 1$) assumption and

$$C_1 = C\left(\frac{\gamma}{\pi}\right)^n \tag{17}$$

is a constant and is canceled out in the calculation of (7). In this paper, the MAP decoder utilizing the Cauchy btp is referred to as the Cauchy-based MAP decoder.

3.3. The Proposed Numerical btp. In order to define the numerical btp, we rewrite (12) as

$$\begin{aligned} \beta_{\alpha,k}(s', s) &= Ce^{(u_k L(u_k)/2)} \prod_{l=1}^{n} f_\alpha(y_{kl} - x_{kl}) \\ &= Ce^{(u_k L(u_k)/2)} \exp\left\{ \sum_{l=1}^{n} \ln[f_\alpha(y_{kl} - x_{kl})] \right\}, \end{aligned} \tag{18}$$

where β_α and f_α are the btp and the pdf, respectively, for SαS noise with characteristic exponent α. Despite the nonexistence of a closed-form expression, $f_\alpha(y_{kl} - x_{kl})$ can be computed numerically based on (4). Suppose that $f_\alpha(\xi)$ can be approximated to within some acceptable tolerance by an integral over a finite interval

$$f_\alpha(\xi) \approx \frac{1}{2\pi} \int_{-\pi L}^{\pi L} \exp(-\gamma|\omega|^\alpha) e^{-j\omega\xi} d\omega. \tag{19}$$

By subdividing $[-\pi L, \pi L]$ into N subintervals of length $2\pi L/N$ and choosing partition points $\omega_m = 2\pi mL/N$ for $m = -(N/2), -(N/2-1), \ldots, -1, 0, 1, \ldots, (N/2-2), (N/2-1)$, $f_\alpha(\xi)$ can be obtained by a Riemann sum

$$\begin{aligned} f_\alpha(\xi) &\approx \frac{1}{2\pi} \sum_{m=-(N/2)}^{N/2-1} \exp\left(-\gamma \left| \frac{2\pi mL}{N} \right|^\alpha \right) e^{-2\pi jmL\xi/N} \left(\frac{2\pi L}{N} \right) \\ &= \frac{L}{N} \sum_{m=-(N/2)}^{N/2-1} \exp\left(-\gamma \left| \frac{2\pi mL}{N} \right|^\alpha \right) e^{-2\pi jmL\xi/N}. \end{aligned} \tag{20}$$

If $f_\alpha(\xi)$ is sampled at intervals of $1/L$ at sampling points $n = 0, \pm 1, \pm 2, \ldots$, (20) can be written as

$$f_\alpha\left(\frac{n}{L}\right) \approx \frac{L}{N} \sum_{m=-(N/2)}^{N/2-1} \exp\left(-\gamma \left| \frac{2\pi mL}{N} \right|^\alpha \right) e^{-2\pi jmn/N}. \tag{21}$$

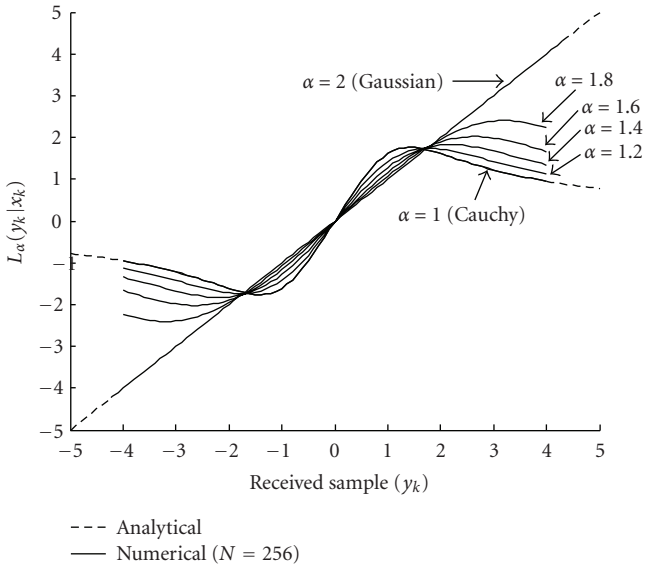

FIGURE 2: $L_\alpha(y_k \mid x_k)$ for different values of α using the analytical and numerical ($N = 256$) methods.

The sum on the right of (21) has the form of a discrete Fourier transform; therefore, it has period N in the variable n. However, the pdf $f_\alpha(n/L)$ does not have period N. To keep the tolerance at an acceptable range, $|n| \leq N/8$ is commonly used [17]. This implies that N meets $N \geq 8L \times \max$, where max is the largest value of $|y_{kl} - x_{kl}|$ and L is chosen large enough such that the area under the characteristic function beyond the range $-\pi L$ to πL is small and can be neglected. The computational complexity is $2N$ operations for every $f_\alpha(n/L)$, where N determines the accuracy of the numerical method. However, by computing $f_\alpha(\xi)$ in advance for a desired range and storing the result in a lookup table, the real time complexity will be as low as one operation per $f_\alpha(n/L)$. Although this prior computation needs $2N^2$ operations, with the aid of the fast Fourier transform (FFT) algorithm and choosing N as a positive integer power of two, the complexity will be reduced to $4N\log_2(N)$ arithmetic operations. In the next section, we show, through simulation results, that $N = 256$ yields highly accurate results. This means that with today's advancement in computer and VLSI technology, it is feasible to implement the proposed numerical method in practical systems.

Referring back to the definition of the numerical btp, although the second line of (18) seems unnecessary, it is needed when converting the resultant MAP algorithm to the Log-MAP algorithm [18]. In fact, the rest of the modification is similar to that of [18] and thus is omitted for the sake of brevity. The Log-MAP algorithm gives a performance identical to that of the MAP algorithm, but at a fraction of its complexity. Hence, it is preferred over the MAP algorithm in practice.

4. Results and Discussion

4.1. Comparative Analysis. The difference between the three aforementioned btps lies in the numerical calculation of the conditional probabilities $f_\alpha(y_{kl} - x_{kl})$. Therefore, the resultant MAP decoding algorithms can be compared by studying the conditional LLR which is defined as

$$L_\alpha(y_k \mid x_k) = \ln\left(\frac{P_\alpha(y_k \mid x_k = +1)}{P_\alpha(y_k \mid x_k = -1)}\right) = \ln\left(\frac{f_\alpha(y_k - 1)}{f_\alpha(y_k + 1)}\right), \tag{22}$$

where y_k is the receiver's matched filter output. The sign of $L_\alpha(y_k \mid x_k)$ indicates whether the transmitted bit x_k is more likely to be $+1$ or -1, and its magnitude gives an indication of how likely its sign gives the correct value of x_k. For Gaussian ($\alpha = 2$) and Cauchy ($\alpha = 1$) distributions, the conditional LLR can be expressed in closed form as

$$\begin{aligned} L_2(y_k \mid x_k) &= \ln\left(\frac{f_2(y_k - 1)}{f_2(y_k + 1)}\right) \\ &= \left(-\frac{1}{4\gamma}(y_k - 1)^2\right) - \left(-\frac{1}{4\gamma}(y_k + 1)^2\right) \\ &= \frac{y_k}{\gamma}, \end{aligned} \tag{23}$$

$$\begin{aligned} L_1(y_k \mid x_k) &= \ln\left(\frac{f_1(y_k - 1)}{f_1(y_k + 1)}\right) \\ &= \ln\left(\frac{\left(\gamma^2 + (y_k + 1)^2\right)}{\left(\gamma^2 + (y_k - 1)^2\right)}\right), \end{aligned} \tag{24}$$

respectively. Figure 2 shows the analytical and numerical $L_\alpha(y_k \mid x_k)$ results for several values of α, from 1 to 2, using $\gamma = 1$, where $N = 256$ is used in the numerical method.

From Figure 2, it is clear that the proposed numerical method agrees well with the analytical results, as exemplified by $L_1(y_k \mid x_k)$ and $L_2(y_k \mid x_k)$, for Cauchy ($\alpha = 1$) and Gaussian ($\alpha = 2$), respectively. It confirms that the numerical method with $N = 256$ can produce very accurate results for $\alpha = 1$ and $\alpha = 2$, which also implies the accuracy of the numerical method with $N = 256$, for $1 < \alpha < 2$. Figure 2 also illustrates the limitation of the Gaussian-based MAP algorithm in impulsive noise, as $L_2(y_k \mid x_k)$ increases linearly with y_k. Other $L_\alpha(y_k \mid x_k)$ for $\alpha < 2$ are nonlinear, which can suppress outlying y_k and act as a protection mechanism against impulses. This difference between $L_2(y_k \mid x_k)$ and $L_{\alpha<2}(y_k \mid x_k)$ explains the poor performance of the classical Gaussian-based turbo decoder in the presence of impulsive noise. This is also consistent with findings in [11–13], where Cauchy-based receivers were reported to perform relatively well in impulsive environments.

In order to heuristically illustrate the advantage of the proposed numerical btp over the Gaussian and Cauchy btps in non-Cauchy impulsive noise, we examine the APP-LLR outputs generated by the MAP decoder using the Gaussian, Cauchy, and numerical btps in impulsive SαS noise ($\alpha = 1.7$). Figure 3 shows the APP-LLR outputs for 250 symbols taken from the second component decoder where the channel E_b/N_0 is 4 dB. The encoder input is a string of all +1 s;

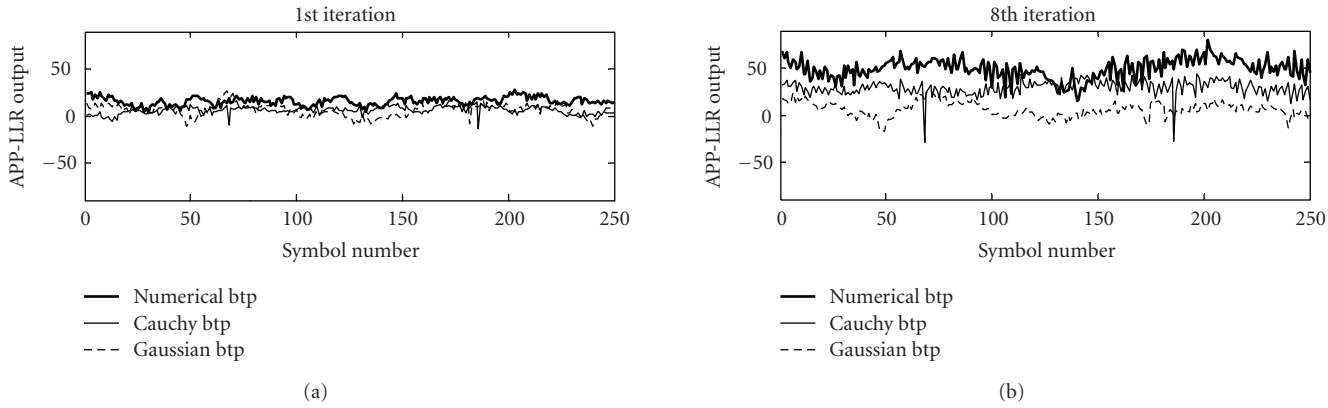

Figure 3: APP-LLR outputs from the second MAP decoder using Gaussian, Cauchy and numerical btps in impulsive SαS noise ($\alpha = 1.7$).

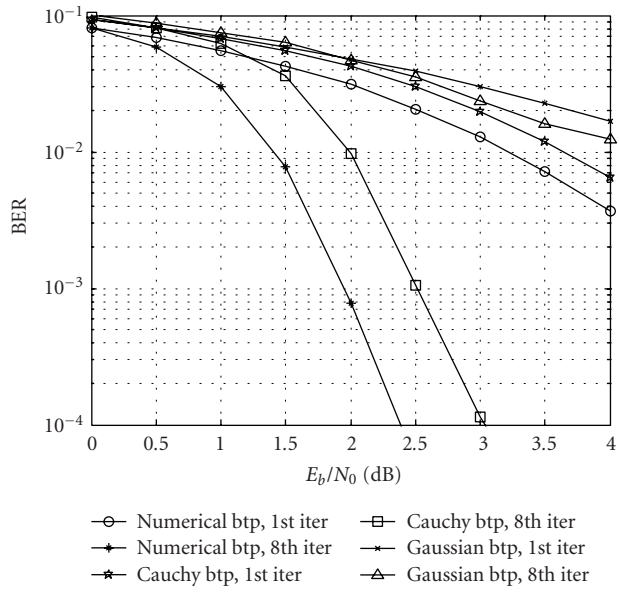

Figure 4: BER performance of the rate-1/3 MAP decoder using Gaussian, Cauchy and numerical btps in impulsive SαS noise ($\alpha = 1.7$).

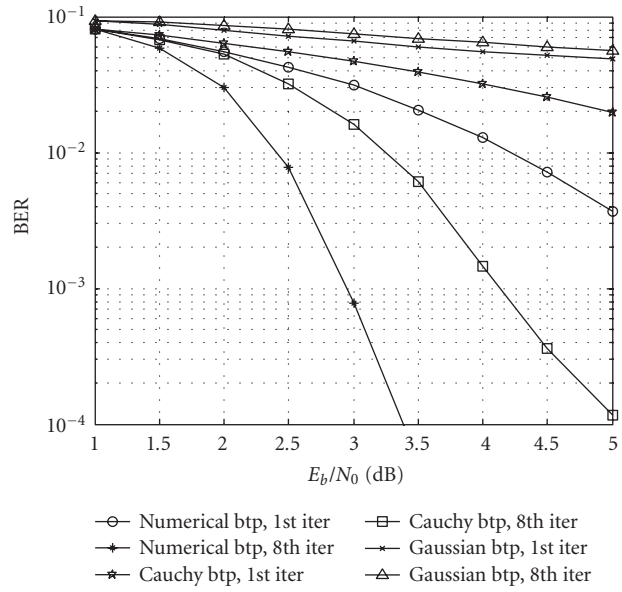

Figure 5: BER performance of the rate-1/3 MAP decoder using Gaussian, Cauchy and numerical btps in impulsive SαS noise ($\alpha = 1.3$).

hence, positive APP-LLR values correspond to correct hard decisions.

As seen in Figure 3, a large number of the APP-LLR outputs created by the MAP decoder using the Gaussian btp are negative valued in the first iteration and most of them remain negative valued even at the eighth iteration. This predicts a very poor performance for the Gaussian-based MAP decoder in such an environment. Although the MAP decoder with the Cauchy btp has achieved better results, a few erroneous decisions are observed as spikes, leading to unsatisfactory performance. On the contrary, the numerical btp has greatly influenced the MAP decoder where it is observed that after eight iterations the generated APP-LLR outputs improve in strength progressively towards error-free decisions.

4.2. Performance Comparison of btps. Numerical performance results are obtained in terms of bit error rate (BER) versus the E_b/N_0 for SαS noise (5) in decibels. Information bits are encoded using a rate-1/3 turbo code with constituent encoders having a constraint length of three ($G_0 = 7$, $G_1 = 5$), and a random interleaver of size 1024 bits is used. Results are obtained for up to eight iterations for the MAP decoder utilizing the Gaussian, Cauchy, and numerical btps, but only results for the first and eighth iterations are shown.

4.2.1. Performance in Non-Cauchy Impulsive SαS Noise with $\alpha = 1.7$ and $\alpha = 1.3$. Figure 4 shows the performance in impulsive SαS noise ($\alpha = 1.7$). It is clear that the conventional Gaussian-based MAP decoder has been paralyzed

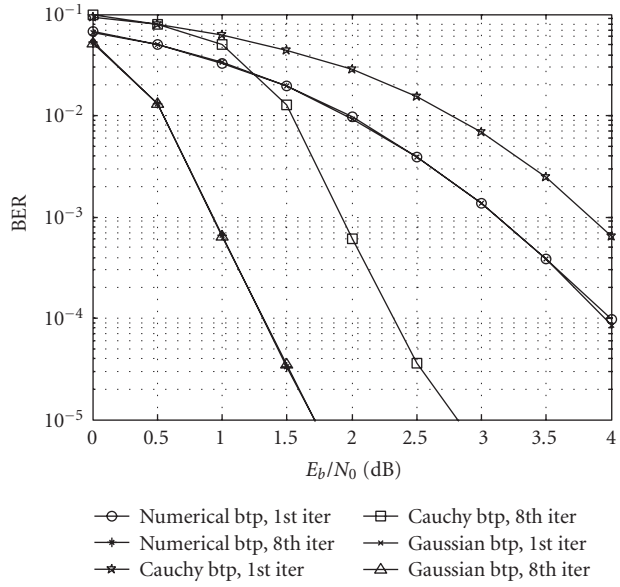

Figure 6: BER performance of the rate-1/3 MAP decoder using Gaussian, Cauchy and numerical btps in Gaussian noise ($\alpha = 2$).

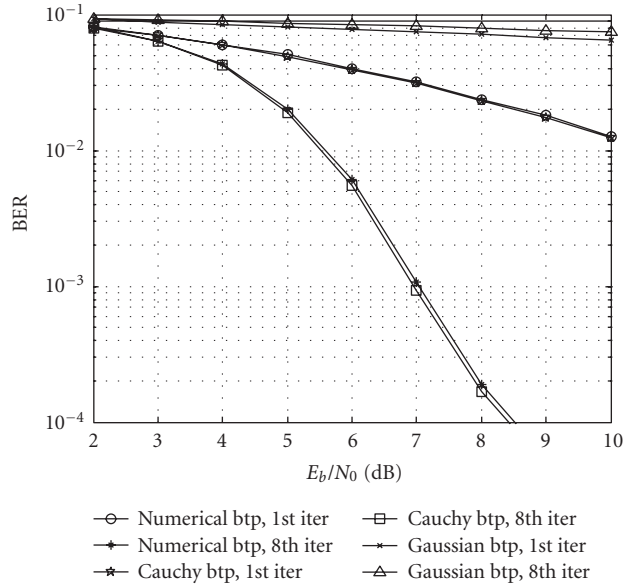

Figure 7: BER performance of the rate-1/3 MAP decoder using Gaussian, Cauchy and numerical btps in Cauchy noise ($\alpha = 1$).

by the impulsive disturbance and almost no performance improvement is gained from the first iteration onwards. However, as expected, the Cauchy-based MAP decoder has achieved better results which has been shown in previous work [11–13]. Ultimately, the MAP decoder furnished with the numerical btp offers better results than the Cauchy-based decoder (by about 0.7 dB), which is valuable for applications requiring reliable data communication at low E_b/N_0 values.

Similar trends are also observed in impulsive channel with $\alpha = 1.3$ in Figure 5, with higher improvement (about 1.65 dB) achieved by using the numerical btp over the Cauchy btp. From Figure 5, it is observed that the Gaussian btp has caused the MAP decoder to produce worse performance as the iteration number increases. This is due to error propagation in the first iteration, which causes the succeeding iterations to suffer more performance degradations.

4.2.2. Performance in Gaussian ($\alpha = 2$) and Cauchy ($\alpha = 1$) Noise. Figure 6 compares the performance in a Gaussian noise ($\alpha = 2$) channel. It can be seen that the numerical btp offers almost identical results as the Gaussian btp which is optimized for this channel. Although we have used an approximate technique to calculate the SαS pdf in our numerical method, the influence on performance is negligible. On the other hand, the Cauchy-based MAP decoder has suffered a performance penalty of 1 dB by assuming that the noise is Cauchy.

Similar comparison is made in Figure 7, albeit in Cauchy noise ($\alpha = 1$). This time, the numerical btp shows almost identical performance as the Cauchy btp and once again is proven to be near optimal. The Gaussian btp, however, has suffered substantial performance degradations.

5. Conclusion

In this paper, we have investigated the decoding of turbo codes using the MAP algorithm in environments impaired by impulsive SαS noise. Due to the non-existence of a closed-form expression for the pdf of SαS noise, a numerical-based btp is proposed for the MAP algorithm to work effectively in impulsive SαS noise. The resultant decoder is then compared with the existing Gaussian- and Cauchy-based MAP decoders. Results show that in Gaussian noise channels ($\alpha = 2$), the MAP decoder furnished with the proposed numerical btp achieves almost identical performance to the conventional Gaussian-optimized MAP decoder, but the Cauchy-based MAP decoder fails to provide such near-optimal performance. Similar trends are seen in Cauchy noise ($\alpha = 1$), where the MAP decoder with the proposed numerical btp achieves near-optimal performance exhibited by the Cauchy-based decoder, but the Gaussian-based MAP decoder is paralyzed by the impulsive disturbance. In non-Cauchy impulsive noise channels ($\alpha < 2$, $\alpha \neq 1, 2$), however, the MAP decoder utilizing the numerical btp substantially outperforms the conventional Gaussian-based MAP decoder and offers better results than the Cauchy-based MAP decoder.

The complexity of the proposed numerical method can be surmounted by the use of the FFT algorithm and a lookup table. Furthermore, the resultant MAP algorithm can be modified to obtain the Log-MAP algorithm using the conventional approach used in [18]. Thus, the MAP decoder with the proposed numerical btp can be used in applications requiring reliable data communication at very low E_b/N_0 values in impulsive noise, such as power-line communications, for which the impulsive noise is well modeled as SαS noise [14].

Acknowledgments

This research was sponsored in part by the Ministry of Science, Technology and Innovation under the Science Fund Grant 01-02-01-SF0074 and by Telekom Malaysia Research & Development under Grant RDTC/100760.

References

[1] C. Berrou, A. Glavieux, and P. Thitimajshima, "Near SHANNON limit error-correcting coding and encoding: turbo-codes," in *Proceedings of the IEEE International Conference on Communications*, pp. 1064–1070, Geneva, Switzerland, 1993.

[2] C. P. Shah, C. C. Tsimenidis, B. S. Sharif, and J. A. Neasham, "Low complexity iterative receiver design for shallow water acoustic channels," *EURASIP Journal on Advances in Signal Processing*, vol. 2010, Article ID 590458, 13 pages, 2010.

[3] R. Lin, P. A. Martin, and D. P. Taylor, "Cooperative signaling with soft information combining," *Journal of Electrical and Computer Engineering*, vol. 2010, Article ID 530190, 5 pages, 2010.

[4] L. Ye and A. Burr, "Separate turbo code and single turbo code adaptive OFDM transmissions," *EURASIP Journal on Wireless Communications and Networking*, vol. 2009, Article ID 609386, 7 pages, 2009.

[5] R. J. Barton and M. Daniel, "Performance evaluation of non-Gaussian channel estimation techniques on ultrawideband impulse radio channels," *International Journal of Communication Systems*, vol. 20, no. 6, pp. 723–741, 2007.

[6] M. Zimmermann and K. Dostert, "Analysis and modeling of impulsive noise in broad-band powerline communications," *IEEE Transactions on Electromagnetic Compatibility*, vol. 44, no. 1, pp. 249–258, 2002.

[7] D. B. Levey and S. McLaughlin, "The statistical nature of impulse noise interarrival times in digital subscriber loop systems," *Signal Processing*, vol. 82, no. 3, pp. 329–351, 2002.

[8] S. A. Kassam, *Signal Detection in Non-Gaussian Noise*, Springer, New York, NY, USA, 1988.

[9] V. Kontorovich and V. Lyandres, "Impulsive noise: a nontraditional approach," *Signal Processing*, vol. 51, no. 2, pp. 121–132, 1996.

[10] C. L. Nikias and M. Shao, *Signal Processing with Alpha-Stable Distributions and Applications*, John Wiley & Sons, New York, NY, USA, 1995.

[11] G. A. Tsihrintzis and C. L. Nikias, "Incoherent receivers in alpha-stable impulsive noise," *IEEE Transactions on Signal Processing*, vol. 43, no. 9, pp. 2225–2227, 1995.

[12] J. How, D. Hatzinakos, and A. N. Venetsanopoulos, "Performance of fh ss radio networks with interference modeled as a mixture of gaussian and alpha-stable noise," *IEEE Transactions on Communications*, vol. 46, no. 4, pp. 509–520, 1998.

[13] M. R. Souryal, E. G. Larsson, B. Peric, and B. R. Vojcic, "Soft-decision metrics for coded orthogonal signaling in symmetric alpha-stable noise," *IEEE Transactions on Signal Processing*, vol. 56, no. 1, pp. 266–273, 2008.

[14] T. C. Chuah, "On reed-solomon coding for data communications over power-line channels," *IEEE Transactions on Power Delivery*, vol. 24, no. 2, pp. 614–620, 2009.

[15] J. G. Gonzalez, J. L. Paredes, and G. R. Arce, "Zero-order statistics: a mathematical framework for the processing and characterization of very impulsive signals," *IEEE Transactions on Signal Processing*, vol. 54, no. 10, pp. 3839–3851, 2006.

[16] L. R. Bahl, J. Cocke, F. Jelinek, and J. Raviv, "Optimal decoding of linear codes for minimizing symbol error rate (Corresp.)," *IEEE Transactions on Information Theory*, vol. 20, no. 2, pp. 284–287, 1974.

[17] P. V. O'neil, *Advanced Engineering Mathematics*, Thomson, 2007.

[18] P. Robertson, E. Villebrun, and P. Hoeher, "Comparison of optimal and sub-optimal MAP decoding algorithms operating in the log domain," in *Proceedings of the IEEE International Conference on Communications*, pp. 1009–1013, June 1995.